

# Chiral density wave versus pion condensation in the 1+1 dimensional NJL model

Prabal Adhikari<sup>1,\*</sup> and Jens O. Andersen<sup>2,3,†</sup>

<sup>1</sup>*St. Olaf College, Physics Department, 1520 St. Olaf Avenue, Northfield, MN 55057, USA*

<sup>2</sup>*Department of Physics, Faculty of Natural Sciences,  
NTNU, Norwegian University of Science and Technology,  
Høgskoleringen 5, N-7491 Trondheim, Norway*

<sup>3</sup>*Niels Bohr International Academy, Blegdamsvej 17, Copenhagen 2100, Denmark*

(Dated: August 11, 2018)

In this paper, we study the possibility of an inhomogeneous quark condensate in the 1+1 dimensional Nambu-Jona-Lasinio model in the large- $N_c$  limit at finite temperature  $T$  and quark chemical potential  $\mu$  using dimensional regularization. The phase diagram in the  $\mu$ - $T$  plane is mapped out. At zero temperature, an inhomogeneous phase with a chiral-density wave exists for  $\mu > \mu_c$ , where  $\mu_c$  is a critical chemical potential. Performing a Ginzburg-Landau analysis, we show that in the chiral limit, the tricritical point and the Lifschitz point coincide. We also consider the competition between a chiral-density wave and a constant pion condensate at finite isospin chemical potential  $\mu_I$ . The phase diagram in the  $\mu_I$ - $\mu$  plane is mapped out and shows a rich phase structure.

## I. INTRODUCTION

Confinement and the spontaneous breaking of chiral symmetry are two of the most important properties of the vacuum of quantum chromodynamics (QCD). The chiral condensate serves as an (approximate) order parameter for the chiral transition: At sufficiently high temperature or density, quarks are deconfined and chiral symmetry is at least partly restored. At asymptotically high temperature, QCD is a weakly interacting quark-gluon plasma, and at asymptotically high density, QCD is in the color-flavor locked phase and forms a color superconductor [1, 2]. At finite baryon chemical potential, lattice simulations are difficult to perform due to the infamous sign problem so one must use low-energy models for QCD. At low temperature and high density, model calculations indicate that the chiral transition is of first order. This picture of a transition from a phase where chiral symmetry is broken by a homogeneous chiral condensate to a phase where chiral symmetry is (approximately) restored is probably too simplistic. Model calculations also suggest that there is an inhomogeneous phase in a relatively small region in the  $\mu_B$ - $T$  plane including part of the  $\mu_B$  axis. The idea of inhomogeneous phases at low temperature and high density dates back to the work by Fulde and Ferrell, and by Larkin and Ovchinnikov in the context of superconductors [3, 4], density waves in nuclear matter by Overhauser [5], and pion condensation by Migdal [6]. In recent years, inhomogeneous phases have been studied in, for example,

cold atomic gases [7], color superconducting phases [8–10], quarkyonic phases [11, 12], pion condensates [13, 14] as well as chiral condensates [15–26], see Refs. [27, 28] for recent reviews.

In order to solve the problem of inhomogeneous phases in its full generality, one must solve an infinite set of coupled gap equations for the various Fourier modes. This has not been done in three dimensions, but one hopes that a simple ansatz for the inhomogeneity will show many of the same features [28]. Inhomogeneities that have been considered in 3+1 dimensions are, for example, one-dimensional modulations such as chiral-density waves and soliton lattices.

Field theories in 1+1 dimensions have been studied extensively over the years as toy models for QCD since they have several important properties in common. For example, all Nambu-Jona-Lasinio (NJL) type models in 1+1 dimensions are asymptotically free and show spontaneous breakdown of chiral symmetry in the vacuum with a dynamically generated mass scale. It should be pointed out, however, that in the NJL-type models in two dimensions the breakdown of a continuous symmetry only takes place in the large- $N_c$  limit, since the phase fluctuations that would otherwise destroy a chiral condensate are of order  $1/N_c$  [29, 30]. Although one is ultimately interested in 3+1 dimensions, the models in 1+1 dimensions are ideal testing grounds for new techniques. Calculations involving inhomogeneous phases can be found in Refs. [31–40]. One of the most important results in the past decade is the construction of the exact phase diagram of the massive Gross-Neveu model in the large- $N_c$  limit [31, 32].

In Ref. [41], we investigated systematically different regularization schemes in effective models with

\* adhika1@stolaf.edu

† andersen@tf.phys.ntnu.no

inhomogeneous phases. The vacuum energy of the NJL model in 1+1 was calculated in the large- $N_c$  limit in the background of a chiral-density wave. A naive application of for example momentum cutoff regularization or dimensional regularization leads to an incorrect result for the vacuum energy. The problem is that there is a residual dependence on the wavevector  $b$  in the limit where the magnitude  $M$  goes to zero [37, 42]. This unphysical behavior can be remedied by subtracting the vacuum energy of a free Fermi gas after having performed a  $b$ -dependent unitary transformation on the Hamiltonian. We also showed that not all regulators are suited to perform a Ginzburg-Landau (GL) analysis of the tricritical and Lifschitz points; the proof of the equality of certain coefficients of the GL functional sometimes involves integration by parts and requires that the surface term vanishes. This is guaranteed if one uses dimensional regularization, but momentum cutoff regularization fails in certain cases, typically when the GL coefficients are divergent.

In this paper, we apply dimensional regularization and the techniques developed in Ref. [41] to calculate the free energy to leading order in  $N_c$  and map out the phase diagram in the  $\mu$ - $T$  plane both in and away from the chiral limit. We also consider the competition between a constant pion condensate and a chiral density wave at finite isospin. Our work is complementary to the study by Ebert et al [39], where the competition between a constant quark condensate and an inhomogeneous pion condensate was studied at  $T = 0$  as a function of  $\mu$  and  $\mu_I$ .

The paper is organized as follows. In Sec. II, we briefly discuss the NJL model in 1+1 dimensions and we derive the thermodynamic potential at finite temperature and chemical potential using dimensional regularization. In Sec. III, we present the phase diagram and a Landau-Ginzburg analysis of the critical and Lifschitz points. In Sec. IV, we discuss the competition between the chiral density wave and a homogeneous pion condensate. Finally, in Sec. V we summarize our results. In the appendices, we provide the reader with some calculational details of two sum-integrals that are needed to locate the critical point and Lifschitz point. We also discuss the vacuum energy in the special case of a finite pion condensate and a vanishing chiral condensate.

## II. LAGRANGIAN AND THERMODYNAMIC POTENTIAL

The Lagrangian of the NJL model in 1+1 dimensions is

$$\mathcal{L} = \bar{\psi} [i\cancel{\partial} - m_0 + (\mu + \frac{1}{2}\tau_3\mu_I)\gamma^0] \psi + \frac{G}{N_c} [(\bar{\psi}\psi)^2 + (\bar{\psi}i\gamma^5\boldsymbol{\tau}\psi)^2], \quad (1)$$

where  $N_c$  is the number of colors,  $\tau_a$  are the three Pauli matrices ( $a = 1, 2, 3$ ) in isospin space,  $m_0$  is the current quark mass. Moreover  $\psi$  is a color  $N_c$ -plet, a two-component Dirac spinor, and a flavor doublet.

$$\psi = \begin{pmatrix} u \\ d \end{pmatrix}. \quad (2)$$

The  $\gamma$ -matrices are  $\gamma^0 = \sigma_2$ ,  $\gamma^1 = i\sigma_1$ , and  $\gamma^5 = \gamma^0\gamma^1 = \sigma_3$ , where  $\sigma_i$  are the three Pauli matrices ( $i = 1, 2, 3$ ). Here  $\mu_B = 3\mu = \frac{3}{2}(\mu_u + \mu_d)$  is the baryon chemical potential and  $\mu_I = \mu_u - \mu_d$  is the isospin chemical potential, where  $\mu_f$  (with  $f = u, d$ ) are the quark chemical potentials. The Lagrangian (1) is a generalization of the original Gross-Neveu model [43] which has a single quark flavor and a single quark chemical potential. The model (1) has a global  $SU(N_c)$  symmetry and for  $m_0 = \mu_I = 0$ , it is also invariant under  $SU_L(2) \times SU_R(2)$  transformations. For nonzero  $m_0$  and  $\mu_I = 0$ , the latter symmetry is reduced to the group  $SU_I(2)$ . For  $m_0 = 0$  and nonzero  $\mu_I$ , it is reduced to  $U_{I_3L}(1) \times U_{I_3R}(1)$ . Finally, for nonzero  $m_0$  and  $\mu_I$ , the symmetry is reduced to  $U_{I_3}(1)$ .

We next introduce the bosonic fields  $\sigma$  and  $\pi_a$  via

$$\sigma = -2\frac{G}{N_c}\bar{\psi}\psi, \quad (3)$$

$$\pi_a = -2\frac{G}{N_c}\bar{\psi}i\gamma^5\tau_a\psi. \quad (4)$$

The Lagrangian (1) then becomes

$$\mathcal{L} = \bar{\psi} [i\cancel{\partial} - m_0 + (\mu + \frac{1}{2}\tau_3\mu_I)\gamma^0 - \sigma - i\gamma^5\pi_a\tau_a] \psi - \frac{N_c(\sigma^2 + \pi_a^2)}{4G}. \quad (5)$$

The chiral condensate we choose is a chiral-density wave of the form

$$\langle\sigma\rangle = M \cos(2bz) - m_0, \quad (6)$$

$$\langle\pi_3\rangle = M \sin(2bz), \quad (7)$$

where  $b$  is a wavevector. For  $b = 0$ , it reduces to the standard homogeneous condensate. With a nonzero isospin chemical potential, there is also the possibility of a pion condensate  $\Delta$ . For simplicity, we take this to be homogeneous

$$\langle\pi_1\rangle = \Delta. \quad (8)$$

The last term in Eq. (5) is denoted by  $-V_0$ , where  $V_0$  is the tree-level potential. Inserting Eqs. (6)–(8) into  $V_0$  and averaging over the spatial extent  $L$  of the system, we obtain for  $L \rightarrow \infty$

$$V_0 = N_c \frac{M^2 + m_0^2 - 2Mm_0\delta_{b,0} + \Delta^2}{4G}. \quad (9)$$

In the homogeneous case, the tree-level potential reduces to the standard expression  $V_0 = N_c \frac{(M-m_0)^2 + \Delta^2}{4G}$ .

The Dirac operator  $D$  can be written as

$$D = \bar{\psi} \left[ i\rlap{\not{\partial}} + \left( \mu + \frac{1}{2}\tau_3\mu_I \right) \gamma^0 - M e^{2i\gamma^5\tau_3bz} - i\gamma^5\tau_1\Delta \right] \psi. \quad (10)$$

We next redefine the quark fields,  $\psi \rightarrow e^{-i\gamma^5\tau_3bz}\psi$  and  $\bar{\psi} \rightarrow \bar{\psi}e^{-i\gamma^5\tau_3bz}$ , which corresponds to a unitary transformation of the Dirac Hamiltonian,  $\mathcal{H} \rightarrow \mathcal{H}' = e^{i\gamma^5\tau_3bz}\mathcal{H}e^{-i\gamma^5\tau_3bz}$ . The Dirac operator then reads

$$D = \left[ i\rlap{\not{\partial}} + \left( \mu + b'\tau_3 \right) \gamma^0 - M - i\gamma^5\tau_1\Delta \right], \quad (11)$$

where  $b' = (b + \frac{1}{2}\mu_I)$ . Going to momentum space, Eq. (10) can be written as

$$D = \left[ \rlap{\not{p}} + \left( \mu + b'\tau_3 \right) \gamma^0 - M - i\gamma^5\tau_1\Delta \right]. \quad (12)$$

Eq. (12) shows that the effective chemical potential for the  $u$ -quarks is  $\mu + b' = \mu_u + b$ , while for the  $d$ -quarks, it is  $\mu - b' = \mu_d - b$ . It is now straightforward to derive the fermionic spectrum in the background (7)–(8). It is given by the zeros of the Dirac determinant and reads [36, 37]

$$p_{0u} = E_\Delta^- - \mu, \quad p_{0d} = E_\Delta^+ - \mu, \quad (13)$$

$$p_{0\bar{u}} = -(E_\Delta^+ + \mu), \quad p_{0\bar{d}} = -(E_\Delta^- + \mu), \quad (14)$$

where

$$E_\Delta^\pm = \sqrt{E_\pm^2 + \Delta^2}, \quad E_\pm = \sqrt{p^2 + M^2} \pm b'. \quad (15)$$

We note that the spectrum depends on the isospin chemical potential  $\mu_I$  via  $b'$ .

Going to Euclidean space, the one-loop contribution to the thermodynamic potential is given by

$$V_1 = -N_c \sum_{\{P\}} \int \log [P_0^2 + (E_\Delta^\pm)^2], \quad (16)$$

where the sum-integral is defined in Eq. (A1) and a sum over  $\pm$  is implied. Summing over the Matsubara frequencies, we can write

$$V_1 = -N_c \int_p \left\{ E_\Delta^\pm + T \log \left[ 1 + e^{-\beta(E^\pm - \mu)} \right] + T \log \left[ 1 + e^{-\beta(E^\pm + \mu)} \right] \right\}, \quad (17)$$

where the integral is defined in Eq. (A2). The first term in Eq. (17) is ultraviolet divergent and requires regularization. The two contributions from  $E_\Delta^\pm$  to this term are denoted by  $V_\pm^{\text{vac}}$ . The second and third terms which depend on the temperature and the chemical potential are finite.

After integrating over angles and changing variables,  $u = \sqrt{p^2 + M^2}$ , we can write

$$V_\pm^{\text{vac}} = -\frac{N_c (e^{\gamma_E} \Lambda^2)^\epsilon}{\sqrt{\pi} \Gamma(\frac{1}{2} - \epsilon)} \int_M^\infty \sqrt{(u \pm b')^2 + \Delta^2} \times \frac{udu}{(u^2 - M^2)^{\frac{1}{2} + \epsilon}}. \quad (18)$$

We cannot calculate analytically the vacuum energy for nonzero  $\Delta$ . In order to isolate the divergences, we expand the dispersion relations around  $\Delta = 0$  and find appropriate subtraction terms. We can then write

$$V_\pm^{\text{vac}} = V_{\text{div}\pm}^{\text{vac}} + V_{\text{fin}\pm}^{\text{vac}}, \quad (19)$$

where

$$V_{\text{div}\pm}^{\text{vac}} = -\frac{N_c (e^{\gamma_E} \Lambda^2)^\epsilon}{\sqrt{\pi} \Gamma(\frac{1}{2} - \epsilon)} \left[ \int_M^\infty |u \pm b'| + \frac{\Delta^2}{2u} \right] \frac{udu}{(u^2 - M^2)^{\frac{1}{2} + \epsilon}}, \quad (20)$$

$$V_{\text{fin}\pm}^{\text{vac}} = -\frac{N_c (e^{\gamma_E} \Lambda^2)^\epsilon}{\sqrt{\pi} \Gamma(\frac{1}{2} - \epsilon)} \int_M^\infty \left[ E_\Delta^\pm - |u \pm b'| - \frac{\Delta^2}{2u} \right] \frac{udu}{(u^2 - M^2)^{\frac{1}{2} + \epsilon}}. \quad (21)$$

We denote the sum of the two terms in (21) by  $V_{\text{fin}}^{\text{vac}}$ . Note that  $V_{\text{fin}\pm}^{\text{vac}} = 0$  for  $\Delta = 0$ . In the chiral limit,

the solutions to the gap equations  $\frac{\partial V}{\partial M} = \frac{\partial V}{\partial \Delta} = 0$  (with  $V = V_0 + V_1$ ) are  $M \neq 0$  and  $\Delta = 0$  or  $M = 0$

and  $\Delta \neq 0$ . In the latter case, Eqs. (20) and (21) are infrared divergent. The IR divergences of (20) cancel against those of (21). However, they must be regulated separately, which is inconvenient. In Appendix A, we discuss this case.

$V_{\text{div}\pm}^{\text{vac}}$  can now be calculated using dimensional reg-

where the function  $f(M, b')$  is defined by

$$f(M, b') = -\frac{N_c}{\pi} \left[ b' \sqrt{b'^2 - M^2} - M^2 \log \frac{b' + \sqrt{b'^2 - M^2}}{M} \right]. \quad (24)$$

The contribution  $V_{\text{div}\pm}^{\text{vac}}$  to the vacuum energy is independent of  $b$ , while the extra term  $f(M, b')$  in  $V_{\text{div}-}^{\text{vac}}$  arises from the integral  $\int_M^\infty |u - b'|$  where one must distinguish between  $u < b'$  and  $u > b'$ .

Expanding  $V_{\text{div}}^{\text{vac}} = V_{\text{div}\pm}^{\text{vac}} + V_{\text{div}-}^{\text{vac}}$  in powers of  $\epsilon$ , we find

$$V_{\text{div}} = -\frac{N_c}{2\pi} \left( \frac{\Lambda^2}{M^2} \right)^\epsilon \left[ \left( \frac{1}{\epsilon} + 1 \right) M^2 + \frac{1}{\epsilon} \Delta^2 \right] + \theta(b' - M) f(M, b'). \quad (25)$$

Eq. (25) contains poles in  $\epsilon$  that are removed by the renormalization of the the fermion mass  $m_0$  and the

ularization and the result is

$$V_{\text{div}\pm}^{\text{vac}} = \frac{N_c}{4\pi} \left( \frac{e^{\gamma_E} \Lambda^2}{M^2} \right)^\epsilon [M^2 \Gamma(-1 + \epsilon) - \Delta^2 \Gamma(\epsilon)], \quad (22)$$

$$V_{\text{div}-}^{\text{vac}} = V_{\text{div}\pm}^{\text{vac}} + \theta(b' - M) f(M, b'), \quad (23)$$

(inverse) coupling constant  $G$  by making the substitutions  $m_0 \rightarrow Z_{m_0} m_0$  and  $\frac{1}{G} \rightarrow Z_{G^{-1}} \frac{1}{G}$ , where

$$Z_{m_0} = \left[ 1 + \frac{2G}{\pi\epsilon} \right]^{-1}, \quad (26)$$

$$Z_{G^{-1}} = \left[ 1 + \frac{2G}{\pi\epsilon} \right]. \quad (27)$$

Note that  $Z_{G^{-1}} = Z_G^{-1}$  and that the ratio  $\frac{m_0}{G}$  is the same for bare and renormalized quantities since  $Z_{m_0} Z_G^{-1} = 1$ . After renormalization, making the substitutions Eqs. (26) and (27), the vacuum energy  $V = V_0 + V_1$  becomes

$$V = N_c \frac{(M^2 + m_0^2 - 2Mm_0\delta_{b,0}) + \Delta^2}{4G} - \frac{N_c M^2}{2\pi} \left[ \log \frac{\Lambda^2}{M^2} + 1 \right] - \frac{N_c \Delta^2}{2\pi} \log \frac{\Lambda^2}{M^2} + V_{\text{fin}}^{\text{vac}} + \theta(b' - M) f(M, b'). \quad (28)$$

Due to the term  $b' \sqrt{b'^2 - M^2}$  in the function  $f(M, b')$ , the vacuum energy is unbounded from below. For  $m_0 = 0$ , and  $\Delta = M = 0$ ,  $V = -\frac{N_c}{\pi} b'^2$  and depends on  $b'$ , which is unphysical (the special case  $M = 0$  and  $\Delta \neq 0$  is discussed in Appendix B.). The same problem occurs if one uses a momentum cutoff and in [37] it was suggested to subtract the term  $V_{\text{sub}} = -\frac{N_c}{\pi} b'^2 + \frac{N_c}{4\pi} \mu_I^2$ , where the latter is necessary to ensure to correct expression of the vacuum energy in the limit  $b \rightarrow 0$ .<sup>1</sup>

As explained in the introduction, we suggest to subtract the vacuum energy for the system of a free Fermi gas (after a unitary transformation) in order

to obtain a result that is independent of  $b$  in the limit  $M \rightarrow 0$ . Thus we subtract the term

$$V_{\text{sub}} = -\frac{N_c m_0^2}{2\pi} \left[ \log \frac{\Lambda^2}{m_0^2} + 1 \right] + \theta(b' - m_0) f(m_0, b') - \theta\left(\frac{1}{2}\mu_I - m_0\right) f(m_0, b'). \quad (29)$$

Eq. (29) then reduces to  $V_{\text{sub}} = -\frac{N_c}{\pi} b'^2 + \frac{N_c}{4\pi} \mu_I^2$  for  $m_0 = 0$ . Moreover, the first term in Eq. (29) is independent of the parameter  $b$  and the chemical potential  $\mu_I$  and can therefore be omitted. The final result for the vacuum energy is therefore

<sup>1</sup> If one uses an energy cutoff [37], there is no spurious  $b$ -

dependence, but one still has to subtract a term  $V_{\text{sub}} = \frac{N_c}{4\pi} \mu_I^2$ .

$$V = N_c \frac{(M^2 + m_0^2 - 2Mm_0\delta_{b,0}) + \Delta^2}{4G} - \frac{N_c M^2}{2\pi} \left[ \log \frac{\Lambda^2}{M^2} + 1 \right] - \frac{N_c \Delta^2}{2\pi} \log \frac{\Lambda^2}{M^2} + V_{\text{fin}}^{\text{vac}} + \theta(b' - M)f(M, b') - \theta(b' - m_0)f(m_0, b') + \theta(\frac{1}{2}\mu_I - m_0)f(m_0, \frac{1}{2}\mu_I). \quad (30)$$

The finite-temperature term is the second and third terms from (17),

$$V_1^T = -\frac{N_c T}{\pi} \int_0^\infty \left\{ \log \left[ 1 + e^{-\beta(E^\pm - \mu)} \right] + \log \left[ 1 + e^{-\beta(E^\pm + \mu)} \right] \right\} dp. \quad (31)$$

The complete free energy in the large- $N_c$  limit is then given by the sum of Eq. (30) and Eq. (31). In contrast to 3+1 dimensions, we have no experimental input that allows us to determine the constituent quark mass  $m_0$  appearing in the expression for the free energy. Following Ref. [36], we demand that the ratio of the dynamical quark mass  $M$  and the pion mass  $m_\pi$  be the same as in three dimensions for  $\mu = \mu_I = 0$ . Choosing the values  $M = 350$  MeV and  $m_\pi = 140$  MeV, one finds a ratio  $\frac{M}{m_\pi} = \frac{5}{2}$ . Numerically, this corresponds to values  $m_0 = 0.05M_0$ ,  $M = 1.04M_0$ , and  $m_\pi = 0.42M_0$ , where  $M_0$  is the dynamical quark mass for  $m_0 = 0$ . Introducing the dimensionless  $\alpha = \pi \frac{m_0}{M_0}$ , this corresponds to  $\alpha = 0.17$ . In the remainder of the paper we use this value for  $\alpha$ . Moreover, since all contributions to the effective potential and gap equations are proportional to  $N_c$ , we omit this factor in all the numerical work.

We close this section by discussing the running parameters in the model and the solution in the vacuum. The coupling constant  $G$  and the mass parameter  $m_0$  satisfy the renormalization group equations

$$\Lambda \frac{dG}{d\Lambda} = -\frac{4G^2}{\pi}, \quad (32)$$

$$\Lambda \frac{dm_0}{d\Lambda} = -\frac{4m_0G}{\pi}. \quad (33)$$

The solutions are

$$G(\Lambda) = \frac{G(\Lambda_0)}{1 + \frac{4}{\pi} G(\Lambda_0) \log \frac{\Lambda}{\Lambda_0}}, \quad (34)$$

$$m_0(\Lambda) = \frac{m_0(\Lambda_0)}{G(\Lambda_0)} G(\Lambda), \quad (35)$$

where  $\Lambda_0$  is some reference scale. These equations show that the ratio  $\frac{m_0}{G}$  is independent of the scale  $\Lambda$ . We also note that  $\frac{m_0}{G}(\Lambda)$  decreases with  $\Lambda$  showing that the model is asymptotically free.

In the vacuum phase, we have  $\Delta = b = 0$ , and in the chiral limit, the solutions  $M_0$  to the gap equation  $\frac{dV}{dM} = 0$  are either  $M_0 = 0$  or

$$M_0 = \Lambda e^{-\frac{\pi}{4G}}. \quad (36)$$

Using Eq. (32), it is straightforward to verify that  $M_0$  is independent of the renormalization scale  $\Lambda$ . The nonanalytic behavior of  $M_0$  as a function of  $G$  shows that the result is nonperturbative. Using for example the two-particle irreducible action formalism, it can be shown that this result corresponds to the summation of the daisy and superdaisy graphs from all orders of perturbation theory [44, 45]. Using Eq. (36), we can trade the scale  $\Lambda$  for the scale  $M_0$ , which gives

$$V = -\frac{N_c M^2}{2\pi} \left[ \log \left( \frac{M_0^2}{M^2} \right) + 1 \right], \quad (37)$$

in agreement with Ebert et al [37]. It is easy to see that the global minimum of  $V$  is at  $M = M_0$ . In the remainder of this paper, we express all dimensionful quantities in appropriate powers of the dynamically generated mass scale  $M_0$ .

### III. CHIRAL-DENSITY WAVE AND NO PION CONDENSATE ( $\Delta = 0$ )

In the absence of a pion condensate, the vacuum energy (30) reduces to

$$V = N_c \frac{(M^2 + m_0^2 - 2Mm_0\delta_{b,0})}{4G} - \frac{N_c M^2}{2\pi} \left[ \log \frac{\Lambda^2}{M^2} + 1 \right] + \theta(b' - M)f(M, b') - \theta(b' - m_0)f(m_0, b') + \theta(\frac{1}{2}\mu_I - m_0)f(m_0, \frac{1}{2}\mu_I), \quad (38)$$

where we have used that  $V_{\text{fin}}^{\text{vac}} = 0$  for  $\Delta = 0$ . The finite-temperature term is given by Eq. (31) evaluated for  $\Delta = 0$ .

### A. Zero temperature

In the limit  $T \rightarrow 0$  and for vanishing pion condensate,  $\Delta = 0$ , one can obtain analytic results for the density-dependent contributions to the effective potential given by Eq. (31). The contributions from the first term in Eq. (31) are denoted by  $V_{\pm}^{\text{med}}$  and

read

$$V_{\pm}^{\text{med}} = -\frac{N_c}{\pi} \int_0^{\infty} (\mu - E_{\pm}) \theta(\mu - E_{\pm}) dp. \quad (39)$$

The contributions from the second term in Eq. (31) vanish for  $\mu > 0$  and vice versa for  $\mu < 0$ . Without loss of generality we take  $\mu > 0$  in the remainder. The contribution  $V_{+}^{\text{med}}$  is straightforward to compute. After changing variables  $u = \sqrt{p^2 + M^2}$  and noting that the upper limit is  $u_f = \mu - b'$  due to the step function, we find

$$\begin{aligned} V_{+}^{\text{med}} &= -\frac{N_c}{\pi} \int_0^{\infty} (\mu - E_{+}) \theta(\mu - E_{+}) dp \\ &= -\frac{N_c}{\pi} \int_M^{u_f} (\mu - u - b') \frac{u du}{\sqrt{u^2 - M^2}} \\ &= -\frac{N_c}{2\pi} \left[ (\mu - b') \sqrt{(\mu - b')^2 - M^2} - M^2 \log \frac{\mu - b' + \sqrt{(\mu - b')^2 - M^2}}{M} \right] \theta(\mu - b' - M). \end{aligned} \quad (40)$$

We next consider the contribution  $V_{-}^{\text{med}}$ , which is given by

$$V_{-}^{\text{med}} = -\frac{N_c}{\pi} \int_0^{\infty} (\mu - E_{-}) \theta(\mu - E_{-}) dp. \quad (41)$$

Here we must distinguish between several cases.

1.  $M > b'$ . The dispersion relation is shown in the left panel of Fig. 1. In this case, the integration is from  $p = 0$  to  $p_C = p_f = \sqrt{(\mu + b')^2 - M^2}$  or  $u = M$  to  $u = u_f = \mu + b'$ ,

$$V_{-}^{\text{med}} = -\frac{N_c}{\pi} \int_M^{u_f} (\mu - u + b') \frac{u du}{\sqrt{u^2 - M^2}}, \quad (42)$$

where  $\mu > M - b'$ . This yields

$$V_{-}^{\text{med}} = -\frac{N_c}{2\pi} \left[ (\mu + b') \sqrt{(\mu + b')^2 - M^2} - M^2 \log \frac{\mu + b' + \sqrt{(\mu + b')^2 - M^2}}{M} \right] \theta(\mu + b' - M). \quad (43)$$

This contribution is obtained from (40) by the substitution  $b' \rightarrow -b'$ .

2.  $b' > M$ . The dispersion relation is shown in the right panel of Fig. 1 (blue curve). In this case  $E_{-} = b' - \sqrt{p^2 + M^2}$  for  $u < b'$  and  $E_{-} = \sqrt{p^2 + M^2} - b'$  for  $u > b'$ .

- (a) If  $\mu > b' - M$ , the integration is from  $p = 0$  to  $p_C = p_f = \sqrt{(b' + \mu)^2 - M^2}$  or  $u = M$  to  $u = u_f = \mu + b'$ . The green horizontal line indicates the value of the chemical potential and the intersection with the dispersion relation gives the upper limit of integration. This yields

$$\begin{aligned} V_{-}^{\text{med}} &= -\frac{N_c}{\pi} \left[ \frac{1}{2} (\mu + b') \sqrt{(\mu + b')^2 - M^2} - b' \sqrt{b'^2 - M^2} + M^2 \log \frac{b' + \sqrt{b'^2 - M^2}}{M} \right. \\ &\quad \left. - \frac{1}{2} M^2 \log \frac{\mu + b' + \sqrt{(\mu + b')^2 - M^2}}{M} \right] \theta(\mu - b' + M). \end{aligned} \quad (44)$$

- (b) If  $\mu < b' - M$ , the integration is from  $p_A = \sqrt{(b' - \mu)^2 - M^2}$  to  $p_B = p_f = \sqrt{(b' + \mu)^2 - M^2}$  or  $u = b' - \mu$  to  $u = b' + \mu$ . The value of the chemical potential is indicated by the orange line and the intersection with the dispersion relation gives the upper and lower limits of integration. This gives

$$V_-^{\text{med}} = -\frac{N_c}{\pi} \left[ \frac{1}{2}(b' + \mu)\sqrt{(b' + \mu)^2 - M^2} + \frac{1}{2}(b' - \mu)\sqrt{(b' - \mu)^2 - M^2} - b'\sqrt{b'^2 - M^2} \right. \\ \left. - \frac{1}{2}M^2 \log \frac{b' + \mu + \sqrt{(b' + \mu)^2 - M^2}}{b' + \sqrt{b'^2 - M^2}} - \frac{1}{2}M^2 \log \frac{b' - \mu + \sqrt{(b' - \mu)^2 - M^2}}{b' + \sqrt{b'^2 - M^2}} \right] \theta(b' - \mu - M). \quad (45)$$

Combining the different cases discussed above, the result for the full effective potential in the large- $N_c$  limit can be written as

$$V = N_c \frac{(M^2 + m_0^2 - 2Mm_0\delta_{b,0})}{4G} - \frac{N_c M^2}{2\pi} \left[ \log \frac{M^2}{M_0^2} + 1 \right] - \theta(b' - m_0)f(m_0, b') + \theta(\frac{1}{2}\mu_I - m_0)f(m_0, \frac{1}{2}\mu_I) \\ - \frac{N_c}{2\pi} \left[ (\mu + b')\sqrt{(\mu + b')^2 - M^2} - M^2 \log \frac{\mu + b' + \sqrt{(\mu + b')^2 - M^2}}{M} \right] \theta(\mu + b' - M) \\ - \frac{N_c}{2\pi} \left[ |\mu - b'|\sqrt{(\mu - b')^2 - M^2} - M^2 \log \frac{|\mu - b'| + \sqrt{(\mu - b')^2 - M^2}}{M} \right] \theta(|\mu - b'| - M). \quad (46)$$

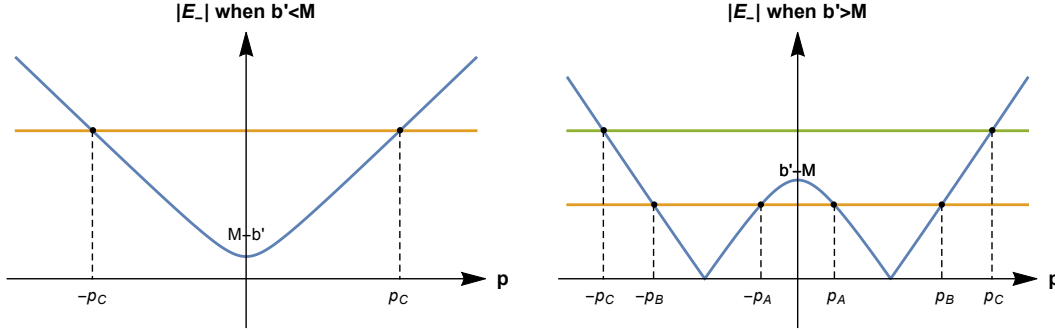


FIG. 1. (Color online) Dispersion relation  $E_-$  for  $\Delta = 0$  (blue curve) for  $b' < M$  (left panel) and for  $b' > M$  (right panel). The horizontal green line is for the case  $\mu > b' - M$  and the horizontal orange line is for the case  $\mu < b' - M$ . See main text for discussion of the regions of integration in the different cases.

In Fig. 2, we show the magnitude  $M$  (blue solid line) and the wavevector  $b$  (red dashed line) both normalized to  $M_0$  as functions of  $\mu/M_0$  at  $\mu_I = T = 0$  for nonzero  $m_0$ . The transition from a constant chiral condensate to a condensate with a nonzero wavevector  $b$  is first order.

Since  $b = b(\mu)$  is larger than  $M = M(\mu)$  in the inhomogeneous phase, it is clear that dispersion relation for the  $u$ -quarks is that shown in the right panel of Fig. 1. This implies that the energy of a  $u$ -quark is zero for the finite momentum  $p_{\min} = \sqrt{b^2 - M^2}$ . This is contrast to the  $d$ -quarks, which are always gapped with a gap  $M + b$ .

## B. Finite temperature

The complete finite-temperature effective potential is given by the sum of the vacuum term (30) and Eq. (31). In Fig. 3, we show the phase diagram in the chiral limit. This phase diagram was first obtained by Ebert et al [37]. The dashed black and red lines indicate second-order transitions, while the solid red line indicates a first-order transition. Note that the phase with nonzero  $M$  and  $b$  extends to infinity for  $T = 0$ . The red dot shows the position of the Lifshitz point whose coordinates in the chiral limit will be given below. The black solid line indicates the

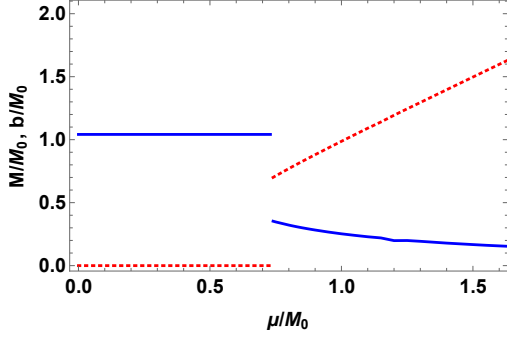


FIG. 2. (Color online) Normalized magnitude of the quark condensate  $M/M_0$  (blue solid line) and wavevector  $b/M_0$  (red dashed line) as functions of  $\mu/M_0$  at  $\mu_I = T = 0$  away from the chiral limit.

first-order transition in the homogeneous case. In the chiral limit, the tricritical point coincides with the Lifshitz point as will be shown below.

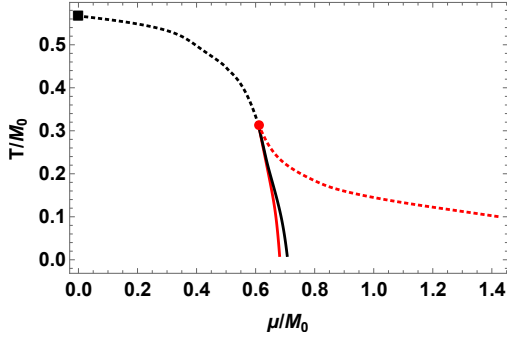


FIG. 3. (Color online) Phase diagram in the chiral limit. The dashed black and red lines indicates a second-order transition, while the solid red line indicates a first-order transition. The red dot indicates the tricritical point which coincides with the Lifshitz point. The solid black line is the first order transition in the homogeneous case.

In Fig. 4, we show the phase diagram away from the chiral limit. Note that the position of the critical point (black) and the Lifshitz point (red) do not coincide, in contrast to the result in the chiral limit. In the chiral limit, the position of the critical end point and the tricritical point can also be found from a Ginzburg-Landau analysis. We then expand the effective potential in powers of  $M$  and derivatives. In the chiral limit, the first few terms of this expansion

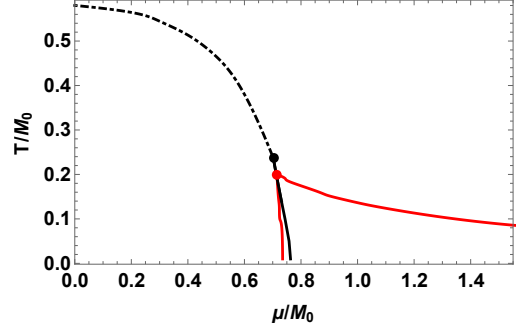


FIG. 4. (Color online) Phase diagram away from the chiral limit. The dashed-dotted line is a crossover and the solid red line is a first-order transition. The black dot indicates the critical end point and the red dot indicates the Lifshitz point, and the solid black line is the first order transition in the homogeneous case.

are

$$V = \frac{N_c M^2}{4G} - 2N_c M^2 \int_{\{P\}} \frac{1}{P^2} + N_c M^4 \int_{\{P\}} \frac{1}{P^4} - \frac{1}{2} N_c (\nabla M)^2 \int_{\{P\}} \frac{p^2 - 3P_0^2}{P^6}. \quad (47)$$

We denote by  $\beta_1$ ,  $\beta_2$  and  $\beta_3$  the coefficients of  $M^2$ ,  $M^4$  and  $(\nabla M)^2$ , respectively. It is easy to show by direct integration over  $p$  or by partial integration, that the coefficients  $\beta_2$  and  $\beta_3$  are equal. The coefficients are equal also if one uses momentum cutoff regularization. This is in contrast to three dimensions where only dimensional regularization [41] or Pauli-Villars regularization [17] yield  $\beta_2 = \beta_3$  due to the absence of surface terms. The tricritical point is given by the condition that the quadratic and quartic terms vanish, and the Lifshitz point is given by the condition that the quadratic and gradient terms vanish. The equality of  $\beta_2$  and  $\beta_3$  implies that the critical point and the Lifshitz point coincide. The condition that these coefficients vanish implies the coupled equations

$$\frac{1}{8G} - \int_{\{P\}} \frac{1}{P^2} = 0, \quad (48)$$

$$\int_{\{P\}} \frac{1}{P^4} = 0. \quad (49)$$

The coefficients  $\beta_i$  ( $i = 1, 2, 3$ ) are all infrared safe since the fermionic Matsubara frequencies are nonzero. If one separates the sum-integrals in a vacuum term and a term that depends on  $T$  and  $\mu$ , they are both divergent in the infrared, but the divergences cancel in the sum. The sum-integral  $\int_{\{P\}} \frac{1}{P^2}$



is also UV divergent and Eq. (48) needs to be renormalized. The sum-integrals appearing in Eqs. (48)–(49) are calculated in Appendix A. Using the expression (A8) and making the substitution  $\frac{1}{G} \rightarrow Z_{G^{-1}} \frac{1}{G}$ , the renormalized version of Eq. (48) reads

$$\frac{1}{8G} - \frac{1}{2\pi} \left[ \log \frac{\Lambda}{2T} + \gamma_E + \text{Li}'_{-2\epsilon_{\text{IR}}}(-e^{-\beta\mu}) + \text{Li}'_{-2\epsilon_{\text{IR}}}(-e^{\beta\mu}) \right] = 0, \quad (50)$$

where  $\Lambda = \Lambda_{\text{UV}}$  and  $\epsilon = \epsilon_{\text{UV}}$ . Using Eq. (36), we can trade  $G$  for  $M_0$  and Eq. (50) can be written as

$$\frac{1}{2\pi} \left[ \log \frac{M_0}{2T} + \gamma_E + \text{Li}'_{-2\epsilon_{\text{IR}}}(-e^{-\beta\mu}) + \text{Li}'_{-2\epsilon_{\text{IR}}}(-e^{\beta\mu}) \right] = 0. \quad (51)$$

Using Eq. (A11), Eq. (49) can be conveniently written as

$$\frac{1}{32\pi^2 T^3} \left[ \psi\left(\frac{1}{2} + \frac{i\mu}{2\pi T}\right) + \psi\left(\frac{1}{2} - \frac{i\mu}{2\pi T}\right) \right] = 0. \quad (52)$$

The solution to Eqs. (51) and (52) gives the position of the Lifschitz point in the  $\mu$ - $T$  plane. The solution is  $(\mu/M_0, T/M_0) = (0.6082, 0.3183)$  and equals the tricritical point in the chiral limit. The position agrees with the numerical result from the phase diagram shown in Fig. 3. In the same manner we can find the critical temperature for the transition at  $\mu = 0$ . Eq. (51) reduces to

$$\frac{1}{2\pi} \left[ \log \frac{M_0}{\pi T} + \gamma_E \right] = 0, \quad (53)$$

whose solution is  $\frac{T}{M_0} = \frac{e^{\gamma_E}}{\pi} \approx 0.567$ . The point  $(0.567, 0)$  is marked with a black square in Fig. 3.

#### IV. CHIRAL-DENSITY WAVE VERSUS HOMOGENEOUS PION CONDENSATE

In this section, we include the possibility of a constant pion condensate.

##### A. Zero temperature

In Fig. 5, we show the normalized quark and pion condensates as functions of the isospin chemical potential divided by  $M_0$  at zero baryon chemical potential and at zero temperature. For  $\mu = 0$ , the wavevector  $b$  vanishes. The pions condense for  $\mu_I \geq \mu_I^c$ , where  $\mu_I^c = m_\pi$  is the pion mass in the vacuum phase. In units of  $M_0$ , this is approximately 0.42. In this phase, the charged pion is a massless

Goldstone bosons associated with the breaking of the  $U_{I_3}(1)$  symmetry. Once the pion condensate starts increasing, the quark condensate drops, which can be thought of as a rotation of the quark condensate into a pion condensate as  $\mu_I$  increases. In the chiral limit, the pion condensate forms for  $\mu_I$  infinitesimally larger than zero and the quark condensate vanishes identically [39]. More generally, in the chiral limit, there is no solution to the gap equations with  $M \neq 0$  and  $\Delta \neq 0$  simultaneously [39].

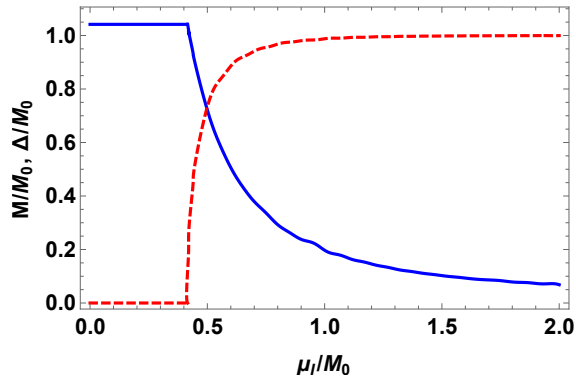


FIG. 5. (Color online) Normalized quark  $M/M_0$  (blue solid line) and pion condensates  $\Delta/M_0$  (red dashed line) as functions of  $\mu_I/M_0$  at  $\mu = T = 0$ .

In Fig. 6, we show the phase diagram for nonzero quark masses in the  $\mu_I$ - $\mu_B$  plane at  $T = 0$ . The values of  $M$ ,  $b$ , and  $\Delta$  are shown for the different regions. The transition from the vacuum phase to the phase with a homogeneous pion condensate is second order. The other transitions are all first order with a jump in the value of  $M$  and possibly a jump in the value of  $b$ . This phase diagram generalizes Fig. 5 of Ref. [36] in which only constant condensates were considered. The phase with  $M \neq 0$  and  $b \neq 0$  for large values of  $\mu$  and small values of  $\mu_I$  replaces the phase with a constant chiral condensate. The region in the lower left corner of the  $\mu$ - $\mu_I$  plane where  $M = M_0$  and  $\Delta = b = 0$  is the vacuum. In this region it can be shown by taking appropriate derivatives of the partition function, that physical quantities are independent of the chemical potentials  $\mu$  and  $\mu_I$ . This is an example of the silver blaze property [46]. As mentioned above, in the chiral limit, the pion condensate forms for  $\mu_I$  infinitesimally small. Thus the vacuum phase reduces to a line along the  $\mu$ -axis.

In the left panel of Fig. 7, we show the condensate  $M/M_0$  as a function of  $\mu_I/M_0$  for  $\mu/M_0 = 0.9$  in the homogeneous case, i.e. we do not allow for a nonzero wavevector  $b$ . The two transitions are of first order.

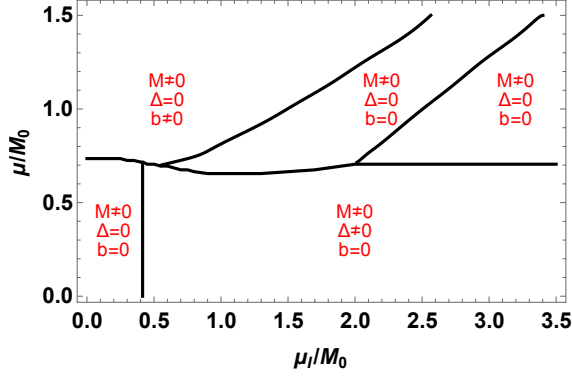


FIG. 6. (Color online) Phase diagram away from the chiral limit. See main text for details.

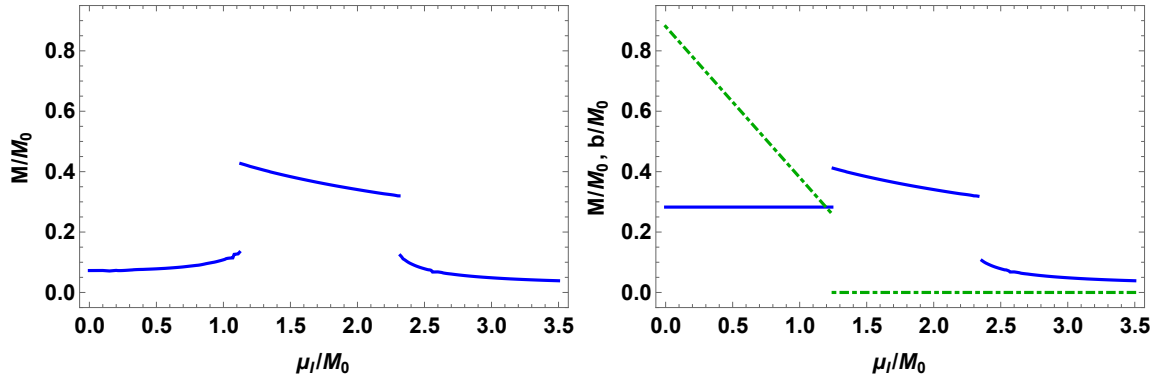


FIG. 7. (Color online) Left panel: Normalized quark condensate  $M/M_0$  at  $T = 0$  as function of  $\mu_I/M_0$  for  $\mu/M_0 = 0.9$  for  $b = 0$ . Right panel: Normalized magnitude of the quark condensate  $M/M_0$  (blue line) and wavevector  $b/M_0$  (green line) at  $T = 0$  as functions of  $\mu_I/M_0$  for  $\mu/M_0 = 0.9$ .

Let us finally discuss the quark and isospin densi-

ties in the different phases. These are given by

$$n_q = -\frac{\partial V}{\partial \mu}, \quad n_I = -\frac{\partial V}{\partial \mu_I}, \quad (54)$$

where  $V = V_0 + V_1$  is the full zero-temperature effective potential. In the phases, where  $\Delta = 0$ , these expressions can be obtained by differentiation of Eq. (46). This yields

$$n_q = \frac{N_c}{\pi} \sqrt{(\mu + b')^2 - M^2} \theta(\mu + b' - M) + \frac{N_c}{\pi} \sqrt{(\mu - b')^2 - M^2} \theta(|\mu - b'| - M) \text{sign}(\mu - b'), \quad (55)$$

$$n_I = \frac{N_c}{2\pi} \sqrt{(\mu + b')^2 - M^2} \theta(\mu + b' - M) - \frac{N_c}{2\pi} \sqrt{(\mu - b')^2 - M^2} \theta(|\mu - b'| - M) \text{sign}(\mu - b') \\ - \frac{N_c}{\pi} \sqrt{b'^2 - m_0^2} \theta(b' - m_0) + \frac{N_c}{\pi} \sqrt{\frac{1}{4}\mu_I^2 - m_0^2} \theta(\frac{1}{2}\mu_I - m_0). \quad (56)$$

In the vacuum phase,  $b = 0$  and so  $b' = \frac{1}{2}\mu_I$ . Moreover,  $M > |\mu \pm \frac{1}{2}\mu_I|$  which implies that  $n_q = n_I = 0$ . This reflects the silver blaze property of the vacuum, namely that its properties are independent of the chemical potential(s) up to some critical value(s) above which there is a phase transition. In the pion-condensed phase, the expressions for  $n_q$  and  $n_I$  follow from (54) and the zero-temperature limit of Eq. (17) (since  $b = 0$ , the subtraction term (29) vanishes) [36]

$$n_q = \frac{N_c}{\pi} \int_0^\infty [\theta(\mu - E_\Delta^+) + \theta(\mu - E_\Delta^-)] dp, \quad (57)$$

$$n_I = \frac{N_c}{2\pi} \int_0^\infty \left[ \frac{E^+}{E_\Delta^+} \theta(E_\Delta^+ - \mu) - \frac{E^-}{E_\Delta^-} \theta(E_\Delta^- - \mu) \right] dp. \quad (58)$$

Since  $E_\Delta^\pm > \mu$  in this phase, we immediately obtain  $n_q = 0$ . The expression for  $n_I$  can be found analytically only in the chiral limit. From Eq. (B5), we find

$$n_I = \frac{N_c}{2\pi} \mu_I. \quad (59)$$

## B. Finite temperature

In Fig. 8, we show the phase diagram for finite quark masses for  $T/M_0 = 0.1$ . The inhomogeneous phase now has become an island which shrinks as the temperature increases further and eventually it disappears. The chiral condensate  $M$  is continuous through the corridor. The two phases with  $M \neq 0$  and  $b = \Delta = 0$  in the upper right part of Fig. 6 have now merged into a single phase. The transitions are all first order.

In Fig. 9, we show the normalized quark condensate  $M/M_0$  and wavevector  $b/M_0$  as functions of  $\mu/M_0$  for  $\mu_I = 0$  and  $T/M_0 = 0.1$ . The two transitions are first order.

In Fig. 10, we show the normalized quark condensate  $M/M_0$  as a function of  $\mu_I/M_0$  for  $\mu/M_0 = 0.9$  and  $T/M_0 = 0.1$  with the restriction of a constant condensate i.e. for  $b = 0$ . In contrast to the case at  $T = 0$ , cf. Fig. 7,  $M/M_0$  is continuous.

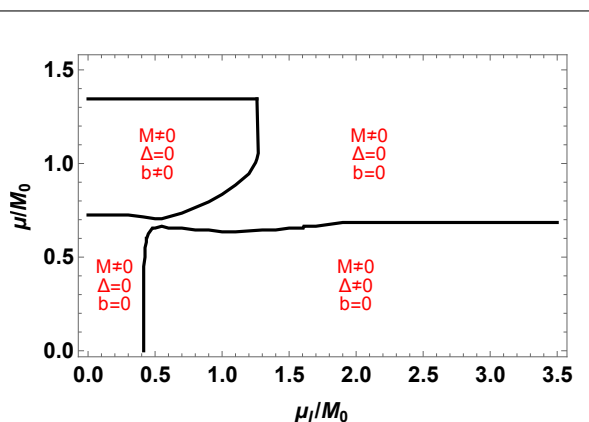


FIG. 8. (Color online) Phase diagram away from the chiral limit for  $T/M_0 = 0.1$ . See main text for details.

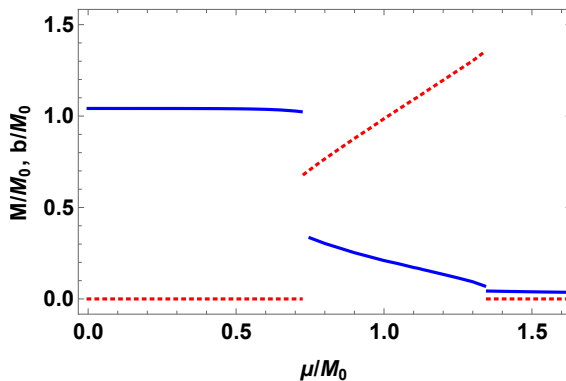


FIG. 9. (Color online) Normalized quark condensate  $M/M_0$  and wavevector  $b/M_0$  as functions of  $\mu/M_0$  for  $\mu_I = 0$  and  $T/M_0 = 0.1$ .

In Fig. 11, we show the normalized quark condensate  $M/M_0$  (blue line) and  $b/M_0$  (green line) as functions of  $\mu_I/M_0$  for  $\mu/M_0 = 0.9$  and  $T/M_0 = 0.1$ .  $M/M_0$  is discontinuous only for one value of  $\mu_I$  showing that the the phases with  $M/M_0 \neq 0$  and  $b = \Delta = 0$  have merged into a single phase, cf. the upper right part of Fig. 8.

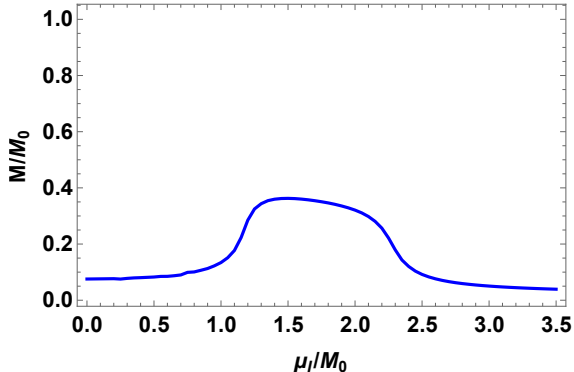


FIG. 10. (Color online) Normalized chiral condensate  $M/M_0$  as a function of  $\mu_I/M_0$  for  $\mu/M_0 = 0.9$  and  $T/M_0 = 0.1$  in the homogeneous case, i.e. we do not allow for nonzero  $b$ .

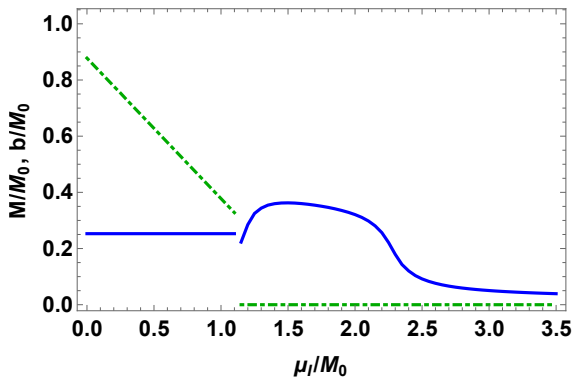


FIG. 11. (Color online) Normalized chiral condensate  $M/M_0$  (blue line) and wavevector  $b/M_0$  (green line) as functions of  $\mu_I/M_0$  for  $\mu/M_0 = 0.9$  and  $T/M_0 = 0.1$ .

## V. SUMMARY

In this paper, we have studied various aspects of the phase diagram of the NJL model in 1+1 dimensions in the large- $N_c$  limit as a function of  $T$ ,  $\mu$ , and  $\mu_I$  using dimensional regularization. The calculations are done with finite quark masses and generalize the results of [36] in which only homogeneous condensates were considered.

We have also carried out a GL analysis of the tricritical and Lifshitz points and derived a set of equations that determine their position in the  $\mu$ - $T$  plane. In the chiral limit they coincide, while they are separated away from it, cf. Figs. 3 and 4. Dimensional regularization proved to be very useful in their calculation since it can be conveniently used to regulate

infrared divergences, which cancel in the final result.

In this paper, we restricted ourselves to a constant pion condensate. The related problem of a constant chiral condensate and an inhomogeneous pion condensate was considered in Ref. [39]. It would be of interest to extend our calculations to allow for spatially modulated chiral and pion condensates at the same time. Eq. (8) would then be replaced by

$$\langle \pi_1 \rangle = \Delta \cos(2kz), \quad \langle \pi_2 \rangle = \Delta \sin(2kz), \quad (60)$$

where  $k$  is another wavevector. One complication that arises in the case of an inhomogeneous pion condensate is that one can no longer find simple analytic expressions for the dispersion relations, which means that the problem must be solved numerically in its entirety. Some work along these lines has been done in the chiral limit by Ebert et al [39], but a complete mapping of the phase diagram with nonzero quark masses is still missing.

## ACKNOWLEDGMENTS

The authors would like to thank the Niels Bohr International Academy for its hospitality. P.A. would like to acknowledge the research travel support provided by the Office of the Dean and the Physics Department at St. Olaf College. P.A. would also like to thank Professor Richard Brown at the Computer Science Department and Tony Skalski for providing computational support.

## Appendix A: Sum-integrals

In this appendix, we evaluate the relevant one-loop sum-integrals that we need. The sum-integral is defined by

$$\not\int_{\{P\}} = T \sum_{\{P_0\}} \int_p \quad (A1)$$

where the integral is defined by

$$\int_p = \left( \frac{e^{\gamma_E} \Lambda^2}{4\pi} \right)^\epsilon \int \frac{d^d p}{(2\pi)^d}, \quad (A2)$$

and  $d = 1 - 2\epsilon$ ,  $P_0 = (2n+1)\pi T + i\mu$  are the fermionic Matsubara frequencies, and  $\Lambda$  is the renormalization scale associated with the  $\overline{\text{MS}}$  scheme.

We first consider the sum-integral

$$I_1 = \not\int_{\{P\}} \frac{1}{P^2}. \quad (A3)$$

After summing over Matsubara frequencies, we can write

$$I_1 = \frac{1}{2} \int_p \frac{1}{p} \left[ 1 - \frac{1}{e^{\beta(p-\mu)} + 1} - \frac{1}{e^{\beta(p+\mu)} + 1} \right], \quad (\text{A4})$$

The first integral in Eq. (A4) which is independent of  $\mu$  and  $T$  has logarithmic divergences in the infrared and in the ultraviolet. The integral vanishes if the same scale is used in the regularization of the ultra-

violet and infrared divergences [47]. If different scales are used, the value of the integral is

$$\int_p \frac{1}{p} = \frac{1}{4\pi} \left[ \frac{1}{\epsilon_{\text{UV}}} - \frac{1}{\epsilon_{\text{IR}}} + \log \frac{\Lambda_{\text{UV}}^2}{\Lambda_{\text{IR}}^2} \right], \quad (\text{A5})$$

where the subscripts UV and IR indicate the different scales. The second and third integrals in Eq. (A4) which depend on  $\mu$  and  $T$  have logarithmic infrared divergences. The integrals can also be calculated in dimensional regularization and read

$$\frac{1}{2} \int_p \frac{1}{p} \left[ \frac{1}{e^{\beta(p-\mu)} + 1} + \frac{1}{e^{\beta(p+\mu)} + 1} \right] = - \left( \frac{e^{\gamma_E} \Lambda_{\text{IR}}^2}{T^2} \right)^{\epsilon_{\text{IR}}} \frac{\Gamma(-2\epsilon_{\text{IR}})}{2\sqrt{\pi}\Gamma(\frac{1}{2} - \epsilon_{\text{IR}})} \left[ \text{Li}_{-2\epsilon_{\text{IR}}}(-e^{-\beta\mu}) + \text{Li}_{-2\epsilon_{\text{IR}}}(-e^{\beta\mu}) \right], \quad (\text{A6})$$

where  $\text{Li}_s(z)$  is the polylogarithmic function with argument  $z$  and the subscript IR indicates the dimensional regularization is used to regulate the infrared divergences. Expanding in powers of  $\epsilon_{\text{IR}}$  to order  $\epsilon_{\text{IR}}^0$  yields

$$\frac{1}{2} \int_p \frac{1}{p} \left[ \frac{1}{e^{\beta(p-\mu)} + 1} + \frac{1}{e^{\beta(p+\mu)} + 1} \right] = -\frac{1}{4\pi} \left[ \frac{1}{\epsilon_{\text{IR}}} + \log \frac{\Lambda_{\text{IR}}^2}{T^2} + 2\gamma_E - 2\log 2 + 2\text{Li}'_{-2\epsilon_{\text{IR}}}(-e^{-\beta\mu}) + 2\text{Li}'_{-2\epsilon_{\text{IR}}}(-e^{\beta\mu}) \right], \quad (\text{A7})$$

where  $\text{Li}'_{-2\epsilon_{\text{IR}}}(-e^{\pm\beta\mu}) = \left. \frac{\partial \text{Li}_{-2\epsilon_{\text{IR}}}(-e^{\pm\beta\mu})}{\partial \epsilon_{\text{IR}}} \right|_{\epsilon_{\text{IR}}=0}$ . Subtracting Eq. (A7) from Eq. (A5), we find

$$I_1 = \frac{1}{4\pi} \left[ \frac{1}{\epsilon_{\text{UV}}} + \log \frac{\Lambda_{\text{UV}}^2}{T^2} + 2\gamma_E - 2\log 2 + 2\text{Li}'_{-2\epsilon_{\text{IR}}}(-e^{-\beta\mu}) + 2\text{Li}'_{-2\epsilon_{\text{IR}}}(-e^{\beta\mu}) \right]. \quad (\text{A8})$$

We note that the poles in  $\epsilon_{\text{IR}}$  cancel. Eq. (A8) simplifies in the case  $\mu = 0$ . Using  $\left. \frac{\partial \text{Li}_{-2\epsilon_{\text{IR}}}(-1)}{\partial \epsilon_{\text{IR}}} \right|_{\epsilon_{\text{IR}}=0} = \frac{1}{2} \log \frac{2}{\pi}$ , we find

$$I_1 = \frac{1}{4\pi} \left[ \frac{1}{\epsilon_{\text{UV}}} + \log \frac{\Lambda_{\text{UV}}^2}{\pi^2 T^2} + 2\gamma_E \right]. \quad (\text{A9})$$

The second sum-integral we need is

$$I_2 = \sum_{\{P\}} \int \frac{1}{P^4}. \quad (\text{A10})$$

$I_2$  is finite in the infrared as well as in the ultraviolet. Integration in  $d = 1$  dimension then yields

$$\begin{aligned} I_2 &= \frac{T}{4} \sum_{n=-\infty}^{n=\infty} \frac{1}{|P_0|^3} \\ &= \frac{1}{32\pi^3 T^2} \sum_{n=-\infty}^{n=\infty} \frac{1}{\left| n + \frac{1}{2} + \frac{i\mu}{2\pi T} \right|^3} \\ &= \frac{1}{32\pi^3 T^2} \left[ \zeta\left(3, \frac{1}{2} + \frac{i\mu}{2\pi T}\right) + \zeta\left(3, \frac{1}{2} - \frac{i\mu}{2\pi T}\right) \right], \end{aligned} \quad (\text{A11})$$

where  $\zeta(n, z)$  is the Hurwitz zeta function.

## Appendix B: Vacuum energy for $M = 0$ , $\Delta \neq 0$

We next show that the vacuum energy is independent of  $b$  in the limit  $M \rightarrow 0$ . We therefore set  $m_0 = M = 0$  (if  $m_0$  is nonzero, so is  $M$ ). The dispersion relation reduces to  $E_{\Delta}^{\pm} = \sqrt{(p \pm b')^2 + \Delta^2}$ .

After integrating over angles, we write the the one-loop cotributions to the effective potential as  $V^{\text{vac}} = V_{\text{div}}^{\text{vac}} + V_{\text{fin}}^{\text{vac}}$ , where

$$V_{\text{div}}^{\text{vac}} = -\frac{2N_c(e^{\gamma_E}\Lambda^2)^\epsilon}{\sqrt{\pi}\Gamma(\frac{1}{2}-\epsilon)} \int_0^\infty \sqrt{p^2 + \Delta^2} p^{-2\epsilon} dp, \quad (\text{B1})$$

$$V_{\text{fin}}^{\text{vac}} = -\frac{N_c(e^{\gamma_E}\Lambda^2)^\epsilon}{\sqrt{\pi}\Gamma(\frac{1}{2}-\epsilon)} \int_0^\infty \left[ \sqrt{(p+b')^2 + \Delta^2} + \sqrt{(p-b')^2 + \Delta^2} - 2\sqrt{p^2 + \Delta^2} \right] p^{-2\epsilon} dp. \quad (\text{B2})$$

Integration gives

$$V_{\text{div}}^{\text{vac}} = \frac{N_c}{2\pi} \left( \frac{e^{\gamma_E}\Lambda^2}{\Delta^2} \right)^\epsilon \Delta^2 \Gamma(-1+\epsilon), \quad (\text{B3})$$

$$V_{\text{fin}}^{\text{vac}} = -\frac{N_c}{\pi} b'^2, \quad (\text{B4})$$

where we have evaluated  $V_{\text{fin}}^{\text{vac}}$  in  $d = 1$  dimensions. The term  $V_{\text{fin}}^{\text{vac}}$  is exactly equal to the subtraction term  $f(0, b')$  and so  $V$  is independent of  $b'$ . After

renormalization and adding the term  $f(0, \frac{1}{2}\mu_I)$ , we find

$$V = \frac{N_c\Delta^2}{4G} - \frac{N_c\Delta^2}{2\pi} \left[ \log \frac{\Lambda^2}{\Delta^2} + 1 \right] - \frac{N_c}{4\pi} \mu_I^2. \quad (\text{B5})$$

For  $\mu_I = 0$ , this result is identical to the vacuum energy (37), which is a consequence of the fact that the vacuum energy depends on the quantity  $M^2 + \Delta^2$ .

- 
- [1] Alford, M. G., A. Schmitt, and K. Rajagopal, Rev. Mod. Phys. **80**, 1455 (2008),
- [2] Fukushima, K., and T. Hatsuda, Rept. Prog. Phys. **74**, 014001 (2011).
- [3] P. Fulde and R. A. Ferrell, Phys. Rev. **135**, A550, (1964).
- [4] A. Larkin and Y. Ovchinnikov, Zh. Eksp. Teor. Fiz. **47**, 1136 (1964).
- [5] A. W. Overhauser, Phys. Rev. Lett. **4**, 415 (1960).
- [6] A. B. Migdal, Rev. Mod. Phys. **50**, 107 (1978).
- [7] K. Maeda, T. Hatsuda, and G. Baym, Phys. Rev. A **87**, 021604 (2013).
- [8] M. G. Alford, J. A. Bowers, and K. Rajagopal, Phys. Rev. D **63**, 074016 (2001).
- [9] R. Anglani, G. Nardulli, M. Ruggieri, and M. Mannarelli, Phys. Rev. D **74**, 074005 (2006).
- [10] L. He, M. Jin, and P.-F. Zhuang, Phys. Rev. D **75**, 036003 (2007).
- [11] T. Kojo, Y. Hidaka, L. McLerran, and R. D. Pisarski, Nucl. Phys. A **843**, 37 (2010); *ibid* **875**, 94, (2011).
- [12] T. Kojo, R. D. Pisarski, and A.M. Tselik, Phys. Rev. D **82**, 074015 (2010).
- [13] L. He, M. Jin, and P. Zhuang, Phys.Rev. D **74**, 036005 (2006).
- [14] C.-F. Mu, L.Y. He, and Y.-X. Liu, Phys. Rev. D **82**, 056006 (2010).
- [15] M. Sadzikowski and W. Broniowski, Phys. Lett. B **488**, 63 (2000).
- [16] E. Nakano and T. Tatsumi, Phys. Rev. D **71**, 114006 (2005).
- [17] D. Nickel, Phys. Rev. D **80**, 074025 (2009).
- [18] D. Nickel, Phys. Rev. Lett. **103**, 072301 (2009).
- [19] S. Carignano, D. Nickel, and M. Buballa Phys. Rev. D **82**, 054009 (2010).
- [20] S. Carignano, M. Buballa, and B.-J. Schaefer, Phys. Rev. D **90**, 014033 (2014).
- [21] H. Abuki, Phys. Lett. **B** 728, 427 (2014).
- [22] J. Braun, S. Finkbeiner, F. Karbstein, and D. Roscher Phys. Rev. D **91**,116006 (2015).
- [23] T.-G. Lee, E. Nakano, Y. Tsue, T. Tatsumi, B. Friman, Phys. Rev. D **92**, 034024 (2015).
- [24] A. Heinz, F. Giacosa, and D. H. Rischke, Nucl.Phys. A **933**, 34 (2015).
- [25] M. Buballa and S. Carignano, Eur. Phys. J. A **52**, 57 (2016).
- [26] A. Heinz, F. Giacosa, M. Wagner, and D. H. Rischke, Phys. Rev. D **93**, 014007 (2016)
- [27] R. Anglani, R. Casalbuoni, M. Ciminale, N. Ippolito, R. Gatto, M. Mannarelli, and M. Ruggieri, Rev. Mod. Phys. **86**, 509 (2014).
- [28] M. Buballa and S. Carignano, Prog. Part. Nucl. Phys. **81**, 39 (2015).
- [29] N. D. Mermin and H. Wagner, Phys. Rev. Lett. **17**, 1133 (1966).
- [30] S. Coleman, Commun. Math. Phys. **31**, 259 (1973).
- [31] O. Schnetz, M. Thies, and K. Urlichs, Annals Phys. **321**, 2604 (2006)
- [32] M. Thies, J. Phys. A **39**, 12707 (2006).
- [33] C. Boehmer, M. Thies, and K. Urlichs, Phys. Rev. D **75**, 105017 (2007).
- [34] G. Basar, G. V. Dunne, and M. Thies, Phys. Rev. D **79**, 105012 (2009).
- [35] G. Basar and G. V. Dunne, Phys. Rev. Lett. **100**, 200404 (2008); Phys. Rev. D **78**, 065022 (2008).
- [36] D. Ebert and K. G. Klimenko, Phys. Rev. D **80**, 125013 (2009).

- [37] D. Ebert, N. V. Gubina, K. G. Klimenko, S. G. Kurbanov, and V. Ch. Zhukovsky, Phys. Rev. D **84**, 025004 (2011).
- [38] V. Ch. Zhukovsky, K. G. Klimenko, and I. E. Frolov, Moscow Univ. Phys. Bull. **65**, 539 (2010).
- [39] N. V. Gubina, K. G. Klimenko, S.G. Kurbanov, and V.Ch. Zhukovsky Phys.Rev. D **86**, 085011 (2012).
- [40] M. Thies, e-Print: arXiv:1603.06218.
- [41] P. Adhikari and J. O. Andersen, arXiv:1608.01097.
- [42] J. O. Andersen and T. Brauner, Phys. Rev. D **81** 096004, (2010).
- [43] D. Gross and A. Neveu, Phys. Rev. D **10**, 3235 (1974).
- [44] G. Aarts, D. Ahrensmeier, R. Baier, J. Berges, and J. Serreau, Phys. Rev. D **66**, 045008 (2002).
- [45] J. O. Andersen, Phys. Rev. D **75**, 065011 (2007).
- [46] T. D. Cohen, Phys. Rev. Lett. **91**, 222001 (2003).
- [47] E. Braaten and A. Nieto, Phys. Rev. D **51**, 6990 (1995).